Materials Research. 2015; 18(2): 292-297
DOI: http://dx.doi.org/10.1590/1516-1439.300614

Corrosion and Wear Resistance of Carbon Films Obtained by Electrodeposition on Ferritic Stainless Steel

***Henrique Ribeiro Piaggio Cardoso*[a]*, Tiago Falcade[a], Sandra Raquel Kunst[b], Célia Fraga Malfatti[a]**

[a]Laboratório de Pesquisa em Corrosão – LAPEC, Universidade Federal do Rio Grande do Sul – UFRGS, Avenida Bento Gonçalves, 9500, Porto Alegre, RS, Brazil
[b]Centro de Ciências Exatas e Tecnológica – CCET, Universidade de Caxias do Sul – UCS, Rua Francisco Getúlio Vargas, 1130, Caxias do Sul, RS, Brazil

Received: June 6, 2014; Revised: March 8, 2015

In improving the corrosion and hardness proprieties of ferritic stainless steel, the use of protective coatings becomes an interesting alternative. In this study, a carbon layer was deposited on AISI 430 by electrodeposition using N,N-dimethylformamide with the addition of an organic dopant as the electrolyte. The AISI 430 stainless steel was pretreated by anodization aiming to optimize the film anchoring. The obtained films were characterized by atomic force microscopy, by scanning electron microscopy and by optical interferometry. The microstructural characterization of the films was obtained by Raman Spectroscopy. The corrosion resistance was evaluated by open circuit potential and by potentiodynamic polarization. The friction test and the scratch test were performed to evaluate the mechanical properties. The Raman spectroscopy showed the presence of an amorphous carbon film. The films improved the corrosion resistance of stainless steel. In addition, on the wear analysis the coating showed a good adhesion on the substrate.

Keywords: *corrosion, tribology, stainless steel, electrodeposition, carbon film*

1. Introduction

Ferritic stainless steel is one of the most important engineering materials due to its low cost and easy mechanical forming. It is an ideal material for a wide range of products, such as kitchenware, interconnections and architectural applications. However, this material shows poor performance in corrosion resistance when compared with austenitic stainless steels. A possible solution to enhance its corrosion resistance is the application of protective films[1-4].

Amorphous carbon coatings have been used in surface treatments due to their high corrosion resistance in several corrosive environments, as well as due to the fact that they are electric conductors[5,6].

Traditional methods for carbon films deposition include physical or chemical vapor phase processes, such as Physical Vapor Deposition (PVD) or Chemical Vapor Deposition (CVD) and their variants[4,7-10]. On the other hand, the deposition of amorphous carbon films by electrodeposition can be considered an alternative process. This technique does not use vacuum and high temperatures. Besides, more complex shapes can be produced with the film[11,12].

In 1992, Namba obtained carbon films by electrodeposition using ethanol as the electrolyte[13]. Following this discovery, Suzuki also made carbon films by electrolysis using a water-ethylene glycol solution[12,14]. A year later, Wang performed the experiment with methanol[15].

The chemical group methyl is better than ethyl because it provokes a faster growth of the film. Another important parameter is the dipole moment: the higher the dipole moment is, the easier it is to obtain C-C sp^3 bonds. These bonds are favorable to make diamond like-carbon (DLC) films. Nowadays, the typical electrolytes used in the electrodeposition of carbon films are acetonitrile (CH_3CN), DMF ($HCON(CH_3)_2$), nitromethane (CH_3NO_2), methanol (CH_3OH), nitroethanol (CH_3CH_2OH) and ethanol (CH_3CH_2OH)[12,16].

In the present study, the objective is to obtain a carbon layer on AISI 430 stainless steel to improve the corrosion and hardness proprieties of this material using the electrodeposition technique with N,N-dimethylformamide (DMF) and organic dopant addition as the electrolyte. In this context, the substrate was pretreated by anodization aiming to optimize the film anchoring.

2. Material and Methods

Ferritic stainless steel (AISI 430) disks with a diameter of 15 mm and a thickness of 0.95 mm were used as substrates. The chemical composition of the substrates is: %C: 0.104, %Cr: 16.08, %Mn: 0.455, %P: 0.0124, %S: <0.001 and %Si: 0.33. The samples were sanded on SiC abrasive paper (# 400–1200) and then mechanically polished using 1 μm alumina. In order to optimize the film anchoring on the substrate, the surface was pretreated by anodization with 150 V between the electrodes (platinum wire as cathode and AISI 430 stainless steel sample as anode) for 10 minutes, at room temperature. An acid electrolyte was used, which is currently in patent process.

The carbon films were obtained on an AISI 430 stainless steel sample (with and without anodizing treatment), with

*e-mail: henrique.piaggio@hotmail.com

the application of a cathodic potential of 1200 V between the electrodes for 24 hours. A graphite plate was used as an anode, which was placed at 7 mm from the cathode. An N,N-dimethylformamide (DMF) with organic dopant was used as an electrolyte. The electrodeposition temperature was kept constant at 20 °C with the use of a thermostatic bath with external water circulation.

Atomic force microscopy (AFM - Shimadzu SPM-9500J3, contact mode), scanning electron microscopy (SEM –Jeol 6060, 20 kV) and optical interferometry Zygo (Zigo New View) were performed to observe the surface morphology of the samples. Raman Spectroscopy (Renishaw inVia Raman, laser 514 nm, laser in 10%, 5 accumulations) was used to obtain the microstructural characterization of the films.

The electrochemical characterization was performed using potentiodynamic polarization curves (Omnimetra Instrumentos PG-3901 potentiostat), and the open circuit potential (OCP) was monitored during one hour. For the electrochemical measurements, a saturated calomel electrode (SCE) was used as a reference, a platinum wire was used as a counter-electrode, and a 1 M ethanol: 0.5 M sulfuric acid solution was used as an electrolyte.

The wear tests were performed on a ball-on-plate tribometer at room temperature and a humidity level of 37%. The wear test was performed with a reciprocal linear motion of a 4.76 mm diameter alumina ball, using a constant force of 0.1 N, a frequency of 1 Hz and a track length of 1.5mm. The linear speed was 3 mm/s and the average Hertzian contact stress was 270.13 MPa.

The scratch test was conducted in a CSM scratch tester, using a Berkocich indenter, a linear force of 3 mN to 500 mN, a pre and post load of 3 mN. The scratch appearance and the critical loads were evaluated by optical microscopy.

3. Results and Discussion

3.1. Morphology study

The preparation of the substrate allowed a relatively regular surface, free of imperfections, as shown on the SEM image (Figure 1) and on the AFM image (Figure 2).

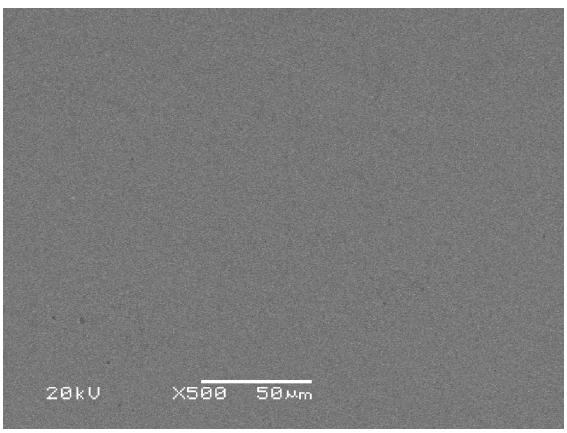

Figure 1. Surface images obtained by SEM of ferritic stainless steel (AISI 430) substrate, after it was mechanically polished.

The low surface roughness was measured, R_a (21.8 nm) and R_z (221.1 nm), as shown in Table 1.

Figure 3 and Figure 4 (image of SEM and AFM) show the anodized surface. This surface acts as an anchorage for the carbon films. By doing so, as expected, the anodized surface presented a high roughness, R_a (199.0 nm) and R_z (3592.3 nm), as shown in Table 1, in comparison to the surface before the anodizing process, which is indicated by the consequent increase on the surface area.

The electrodeposited samples (Figure 5 and Figure 6) showed a lower roughness than the anodized surface, R_a (72.3 nm) and R_z (3290.34 nm), as shown in Table 1. These results indicate that the carbon film grew faster on the valleys than on the peaks, leveling the surface.

Table 1. Comparative table of roughness between the studied systems by optical interferometry.

	R_a [nm]	R_z [nm]
Substrate	21.8 ± 3.5	221.1 ± 38.1
Anodizing	199.0 ± 14.7	3592.3 ± 452.9
Carbon Film	72.3 ± 25.6	3290.3 ± 778.7

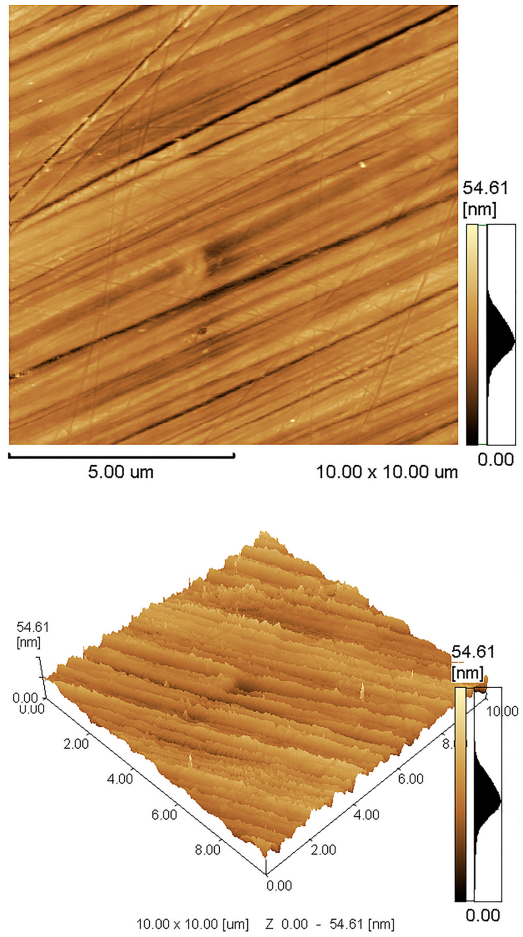

Figure 2. Morphology obtained by AFM of ferritic stainless steel (AISI 430) substrate, after it was mechanically polished. The image on the left shows the top view and the image on the right shows the 3D view of roughness.

3.2. Raman studies

The diamond spectrum has a peak at 1332 cm^{-1} and the graphite spectrum shows a peak at 1580 cm^{-1}[17,18]. In the amorphous carbon films, there are two peaks around 1345–1355 cm^{-1} and 1570–1590 cm^{-1}[18,19], which originated two bands: the G band relates to sp^2 bonding, centered around 1500–1700 cm^{-1} and the D band relates to a bond-angle disorder in the sp^2 caused by the presence of sp^3 bonding, H or N, centered around 1200–1450 cm^{-1}.

The Raman analysis for the obtained carbon film showed two bands centered around 1382.6 ± 1.8 cm^{-1} and

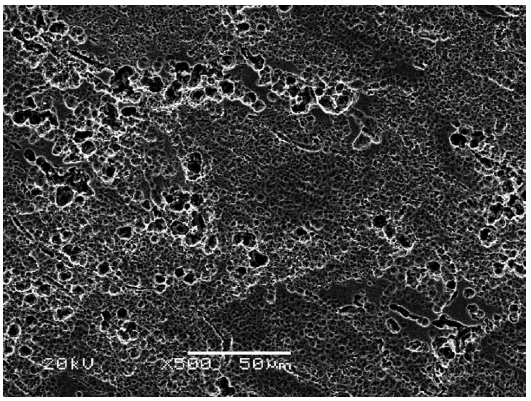

Figure 3. Surface images obtained by SEM of the anodized surface.

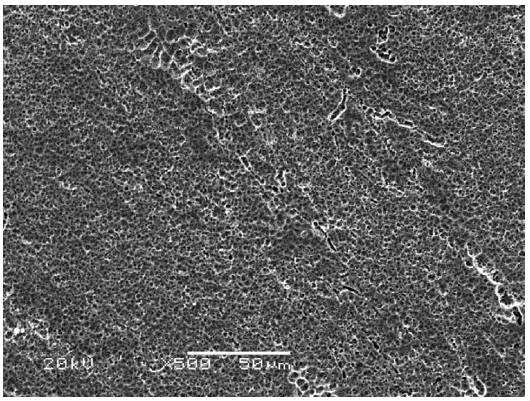

Figure 5. Surface images obtained by SEM of the carbon film on the anodized surface.

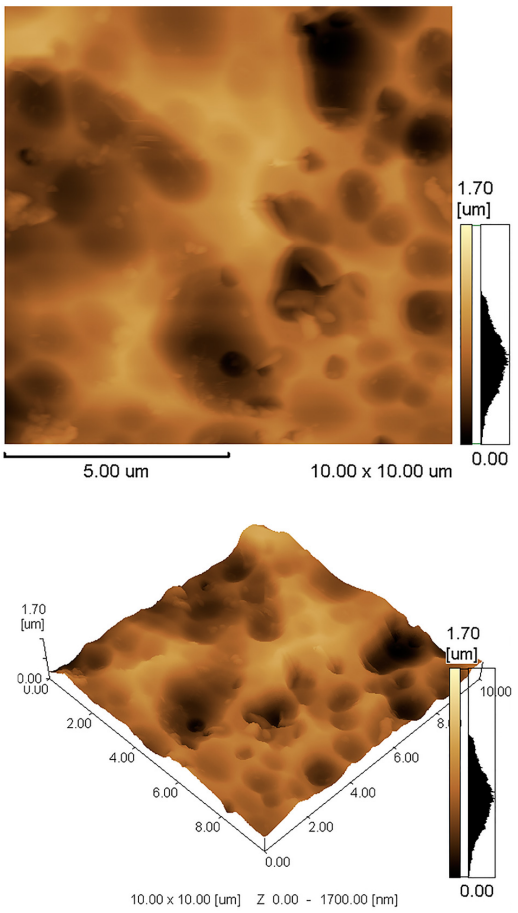

Figure 4. Morphology obtained by AFM of the anodized surface. The image on the left shows the top view and the image on the right shows the 3D view of roughness.

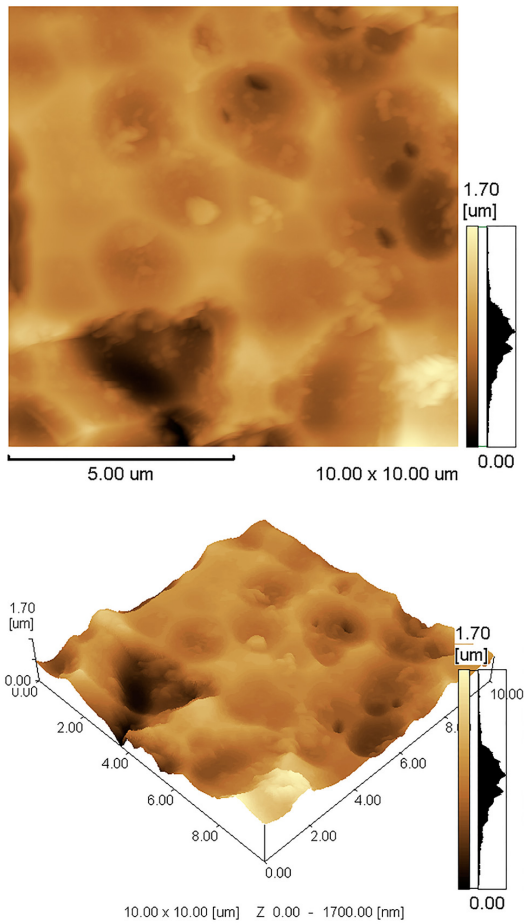

Figure 6. Morphology obtained by AFM of the carbon film on the anodized surface. The image on the left shows the top view and the image on the right shows the 3D view of roughness.

1569.0 ± 1.1 cm^{-1} (Figure 7). This suggests that the structure of these films was composed by mixed sp^2, sp^3 carbon, H and N. In other words, all of the mentioned results are characteristics of amorphous carbon film materials[17,20].

The measured intensity ratio I_D/I_G of the carbon film was 0.68 ± 0.002. This result is the same as the results reported on literature, as per Table 2. The Raman spectrum showed a positive slope of baseline that demonstrates the film has a certain degree of hydrogenation.

3.3. Corrosion behavior

The carbon film offers a significant improvement in corrosion resistance, in a 1 M ethanol and 0.5 M sulfuric acid solution, when compared to an anodized system and even more when compared to a substrate without surface treatment (Figure 8). There was a displacement of the open circuit potential to more noble values, namely: substrate (–512 mV), anodized (36 mV) and carbon film (163 mV).

Furthermore, the anodized system and the carbon film present a considerable reduction in the corrosion current densities, reaching five orders of magnitude higher in relation to the substrate (Figure 9 and Table 3). In addition, the resistance of polarization of film increased four orders of magnitude higher in relation to the substrate. Moreover, the anodizing surface treatment and the film deposition improved de anodic current density, presenting lower values than the uncoated substrate.

This behavior could be associated to the barrier of the oxide film, which forms a physical obstacle amidst the substrate and the corrosive environment. At the same time, the carbon film confers a nobler trait and covers the imperfections and defects of the oxide layer.

3.4. Mechanical behavior

An initial period was observed (Figure 10) with the surfaces sliding freely, and with the coefficient of friction starting at lower values. However, at a subsequent moment of wear, the upper layer was abraded and the coefficient of friction was stabilized at higher values. The oscillation around this average value can be explained by the formation

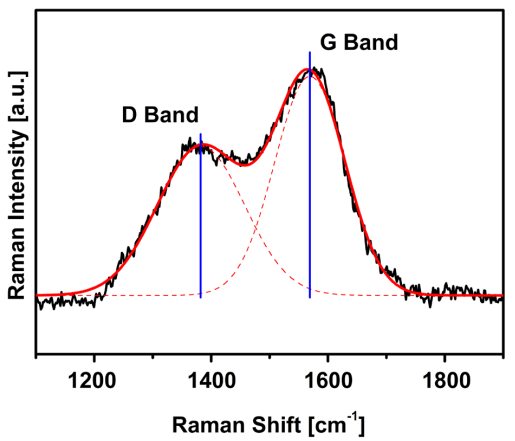

Figure 7. Raman spectral deconvolution of the carbon film and the fitting result.

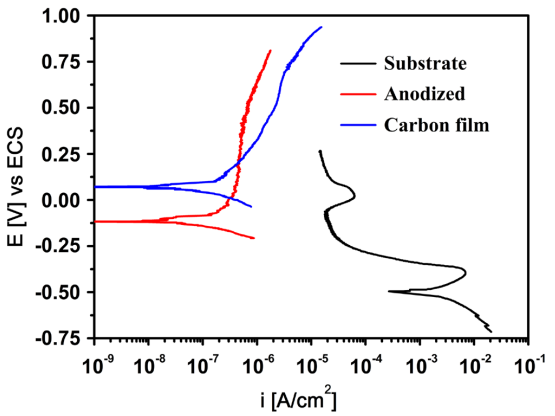

Figure 9. Potentiodynamic polarization curves comparing substrate, anodized and electrodeposited films in a 1 M ethanol and 0.5 M sulfuric acid solution, E vs SCE.

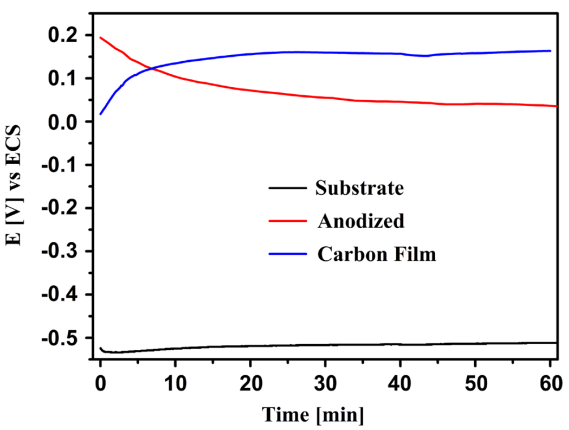

Figure 8. Open circuit potential monitoring in a 1 M ethanol and 0.5 M sulfuric acid solution.

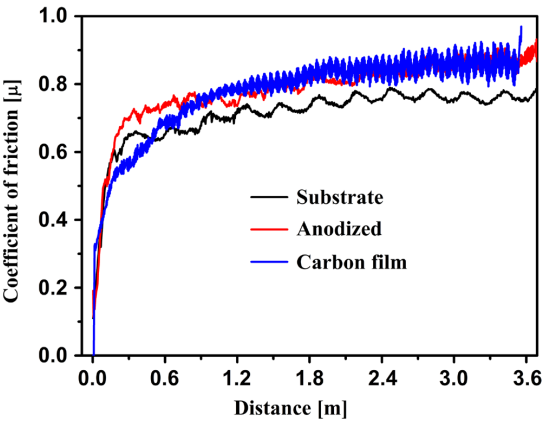

Figure 10. Coefficient of friction in the ball-in-plate test comparing the substrate, the anodized film and the electrodeposited carbon film.

of particles resulting from the contact between the bodies and its insertion in the interface of wear[21].

Finally, it was noted that the coefficient of friction of the polished substrate was lower than the coefficient of the anodized film and the coefficient of the carbon film. This can be explained by the insertion of hard abraded particles for the rougher anodized layer.

The start of the coefficient of friction of the carbon film was lower than of the anodized one, which may be justified by the lubrication characteristic of the carbon film. The carbon film supported the normal load up to 0.72 m, when the value of the coefficient of friction reached the anodized value, indicating that the film is quickly worn.

Figure 11 shows a reduction of wear tracks on the substrate when compared to the carbon film. This suggests that the carbon film and the anodized film absorbed the applied load, which resulted in a less pronounced wear.

The scratch test results show that the film had a plastic deformation in the beginning of the experiment (3 mN, red line in Figure 12) and it had only lateral material displacement in 10 mN (green line in Figure 12). However, the film was not delaminated until the end of the track. This indicates that the coating has adhered well to the substrate.

Table 2. The intensity radio I_D/I_G for the obtained film in comparison with the results presented in the literature.

	Technique	I_D/I_G	Ref
Films obtained by organic liquids on stainless steel (AISI 430)	Electrodeposition	0.68	-
Hard carbon films	PVD techniques	0.32 - 1.62	[8,19]
Films obtained using organic liquids or organic liquids in aqueous solutions	Electrodeposition	0.4 - 2.21	[16,20]
DLC films onto ITO from pure organic liquids	Electrodeposition	2.1	[21]

Table 3. Electrochemical characteristics of the studied systems.

	Substrate	Anodized	Carbon Film
E_{corr} [mV]	–498	–116	69.5
i_{corr} [A/cm^2]	1.63E-06	7.17E-11	8.99E-11
R_p [Ohm/cm^2]	1.60E+04	3.64E+08	2.90E+08

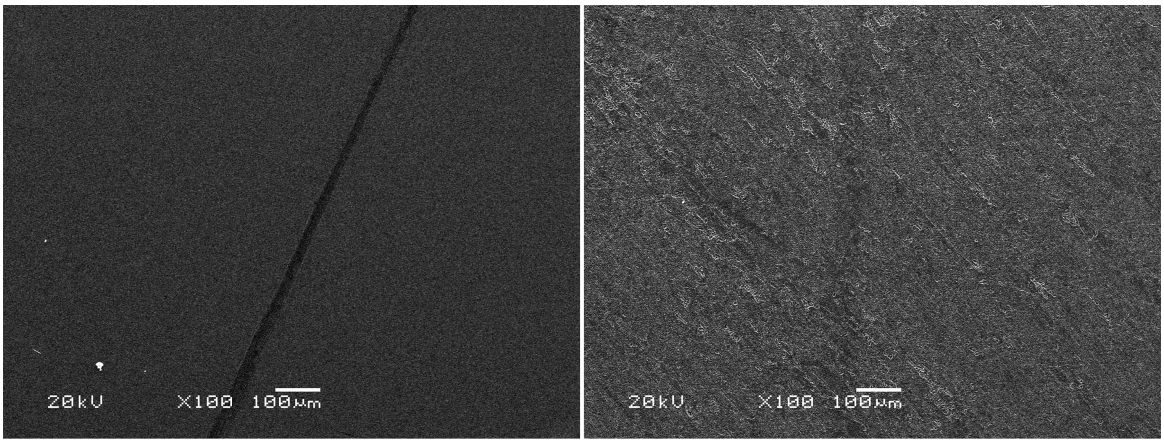

(a) (b)

Figure 11. SEM image of the substrate track (a) and of the carbon film track (b) after wear tests.

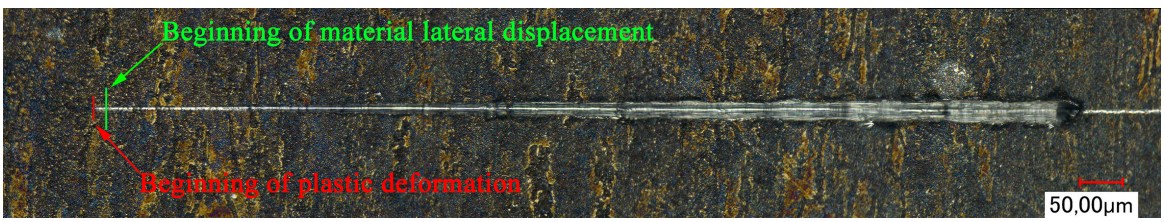

Figure 12. Scratch test image of the carbon film.

4. Conclusions

Before the anodizing process, the substrate had an evenly wrinkled surface. Afterwards, the treatment created a surface that favors the nucleation of the film. Furthermore, the film grew preferentially on anodized valleys, leveling the surface.

The Raman spectroscopy showed the presence of a hydrogenated amorphous carbon film.

The anodized and the carbon film improved the corrosion resistance of stainless steel, diminishing the corrosion, the anodic current densities, and producing a displacement of the corrosion potential to more noble values than the values of the substrate.

In regards to the wear study, this electrodeposited carbon film did not bear the stress for a very long time. However, in the scratch test, the coating showed a good adhesion on the substrate, and the delamination did not occur until the end of the track.

Acknowledgements

The authors would like to thank the Brazilian government agency CNPq for supporting the present research.

References

1. Hsu CH, Lin CK, Huang KH and Ou KL. Improvement on hardness and corrosion resistance of ferritic stainless steel via PVD-(Ti,Cr)N coatings. *Surface and Coatings Technology*. 2013; 231:380-384. http://dx.doi.org/10.1016/j.surfcoat.2012.05.095.
2. Lu HB, Hu Y, Gu MH, Tang SC, Lu HM and Meng XK. Synthesis and characterization of silica–acrylic–epoxy hybrid coatings on 430 stainless steel. *Surface and Coatings Technology*. 2009; 204(1-2):91-98. http://dx.doi.org/10.1016/j.surfcoat.2009.06.035.
3. Chou TP, Chandrasekaran C, Limmer SJ, Seraji S, Wu Y, Forbess MJ, et al. Organic–inorganic hybrid coatings for corrosion protection. *Journal of Non-Crystalline Solids*. 2001; 290(2–3):153-162. http://dx.doi.org/10.1016/S0022-3093(01)00818-3.
4. Silva WM, Carneiro JRG and Trava-Airoldi VJ. XPS, XRD and laser raman analysis of surface modified of 6150 steel substrates for the deposition of thick and adherent diamond-like carbon coatings. *Materials Research*. 2013; 16(3):603-608. http://dx.doi.org/10.1590/S1516-14392013005000027.
5. Falcade T, Shmitzhaus TE, dos Reis OG, Vargas ALM, Hübler R, Müller IL, et al. Electrodeposition of diamond-like carbon films on titanium alloy using organic liquids: Corrosion and wear resistance. *Applied Surface Science*. 2012; 263:18-24. http://dx.doi.org/10.1016/j.apsusc.2012.08.052.
6. Lettington AH. Applications of Diamond-Like Carbon Thin Films. *Philosophical Transactions: Physical Sciences and Engineering*. 1664; 1993(342):287-296.
7. Baranauskas V, Peterlevitz AC, Ceragioli HJ, Souto AL and Durrant SF. Structural properties of diamond and diamond-like carbon grown on stainless-steel blades. *Thin Solid Films*. 2001; 398–399:255-259. http://dx.doi.org/10.1016/S0040-6090(01)01382-7.
8. Lau DWM, Moafi A, Taylor MB, Partridge JG, McCulloch DG, Powles RC, et al. The structural phases of non-crystalline carbon prepared by physical vapour deposition. *Carbon*. 2009; 47(14):3263-3270. http://dx.doi.org/10.1016/j.carbon.2009.07.044.
9. Zhao X, He X, Sun Y, Yi J and Xiao P. Superhard and tougher SiC/diamond-like-carbon composite films produced by electron beam physical vapour deposition. *Acta Materialia*. 2009; 57(3):893-902. http://dx.doi.org/10.1016/j.actamat.2008.10.031.
10. Zhang D, Shen B and Sun F. Study on tribological behavior and cutting performance of CVD diamond and DLC films on Co-cemented tungsten carbide substrates. *Applied Surface Science*. 2010; 256(8):2479-2489. http://dx.doi.org/10.1016/j.apsusc.2009.10.092.
11. Robertson J. Diamond-like amorphous carbon. *Materials Science and Engineering R Reports*. 2002; 37(4–6):129-281. http://dx.doi.org/10.1016/S0927-796X(02)00005-0.
12. Yan XB, Xu T, Yang SR, Liu HW and Xue QJ. Characterization of hydrogenated diamond-like carbon films electrochemically deposited on a silicon substrate. *Journal of Physics D: Applied Physics*. 2004; 37(17):2416-2424. http://dx.doi.org/10.1088/0022-3727/37/17/012.
13. Namba Y. Attempt to grow diamond phase carbon films from an organic solution. *Journal of Vacuum Science & Technology. A, Vacuum, Surfaces, and Films*. 1992; 10(5):3368-3370. http://dx.doi.org/10.1116/1.577829.
14. Suzuki T, Manita Y, Yamazaki T, Wada S and Noma T. Deposition of carbon films by electrolysis of a water-ethylene glycol solution. *Journal of Materials Science*. 1995; 30(8):2067-2069. http://dx.doi.org/10.1007/BF00353035.
15. Wang H, Shen MR, Ning ZY, Ye C, Cao CB, Dang HY, et al. Deposition of diamond-like carbon films by electrolysis of methanol solution. *Applied Physics Letters*. 1996; 69(8):1074. http://dx.doi.org/10.1063/1.116935.
16. Fu Q, Jiu JT, Cao CB, Wang H and Zhu HS. Electrodeposition of carbon films from various organic liquids. *Surface and Coatings Technology*. 2000; 124(2):196-200. http://dx.doi.org/10.1016/S0257-8972(99)00658-1.
17. Zhang J, Huang L, Yu L and Zhang P. Synthesis and tribological behaviors of diamond-like carbon films by electrodeposition from solution of acetonitrile and water. *Applied Surface Science*. 2008; 254(13):3896-3901. http://dx.doi.org/10.1016/j.apsusc.2007.12.029.
18. Tosin M, Peterlevitz A, Surdutovich G and Baranauskas V. Deposition of diamond and diamond-like carbon nuclei by electrolysis of alcohol solutions. *Applied Surface Science*. 1999; 144-145:260-264. http://dx.doi.org/10.1016/S0169-4332(98)00808-3.
19. Cao C, Zhu H and Wang H. Electrodeposition diamond-like carbon films from organic liquids. *Thin Solid Films*. 2000; 368(2):203-207. http://dx.doi.org/10.1016/S0040-6090(00)00765-3.
20. Pang H, Wang X, Zhang G, Chen H, Lv G and Yang S. Characterization of diamond-like carbon films by SEM, XRD and Raman spectroscopy. *Applied Surface Science*. 2010; 256(21):6403-6407. http://dx.doi.org/10.1016/j.apsusc.2010.04.025.
21. Kato K. Wear in relation to friction: a review. *Wear*. 2000; 241(2):151-157. http://dx.doi.org/10.1016/S0043-1648(00)00382-3.